

Application of Thomas Model in the Adsorption of C_4H_8O from 1-Butene flowrate over on SiO_2

Julio Moreno¹, Zaida Borjas¹, Eulises Vargas¹ and Edgar Cuicas²

¹School of Chemical Engineering, Faculty of Engineering, Rafael Urdaneta University, Maracaibo Venezuela.

²Tchemical Department, LDPE Plant, Poliolefinas Internacionales C.A. Los Puertos de Altagracia Venezuela.

Correo electrónico: juliomoreno20@gmail.com, ecuicas@polinter.com.ve

Recibido: 16-02-2021

Aceptado: 12-04-2021

Abstract

Methyl ethyl ketone adsorption over SiO_2 from a 1-butene flowrate has been studied. This research has as a main scope to obtain the kinetic parameter (mass-transfer coefficient), and the adsorption capacity of two towers packed with 9800 kg of silicato remove C_4H_8O from a 1-butene flowrate of 15000 kg/h, placed in a lineal low density polyethylene plant. In each column, two breakthrough curves were constructed by collecting data for the relationship C_o/C_i and plotting the results as a function of time. Thomas model was used to fit the breakthrough curves; obtaining the kinetical parameter (K_f) and the adsorption capacity (Q_o). The breakthrough data collected shows a typical H1 isotherm, the data analysis exhibit a strong relationship between the K_f and Q_o with the methyl ethyl ketone initial concentration (C_i) and weak time dependence for the same parameters. The model selected (Thomas) fits fairly well the data in a range from 0,1 to 0,3 of relative concentration.

Key words: Breakthrough time, adsorption capacity, global mass-transfer coefficient.

Aplicación del Modelo de Thomas para adsorción de C_4H_8O de una corriente de 1-Buteno sobre SiO_2

Resumen

El objetivo principal de esta investigación fue estudiar la adsorción de metil-etil-cetona sobre oxido de silicio para obtener el coeficiente de transferencia de masa K_f y la capacidad de adsorción Q_o de dos torres de adsorción ubicadas en una planta de producción de polietileno lineal de baja densidad empacadas con 9800 kg de SiO_2 , para remover C_4H_8O de una corriente 15000 kg/h de 1-buteno. En cada una de las columnas se construyeron 2 curvas de ruptura a través de la recolección de datos para obtener la relación C_o/C_i en función del tiempo. Con estos datos, el modelo de Thomas fue aplicado para ajustar y obtener el coeficiente de transferencia de masa y de capacidad de adsorción. Las curvas de ruptura mostraron figura típica de una isoterma de adsorción H1 y una fuerte relación entre K_f y Q_o con la concentración inicial de C_4H_8O , así como una débil dependencia del tiempo para los parámetros anteriores. El modelo de Thomas, ajusta bien los datos en el rango de 0,1 a 0,3 C_o/C_i o concentración relativa.

Palabras clave: Tiempo de ruptura, capacidad de adsorción, adsorción, coeficiente global de transferencia de masa.

Introduction

One of the most used technics to control polymer properties is by the addition of a comonomer during the reaction stage, that unsaturated hydrocarbon reacts with me monomer producing a copolymer with some specific characteristics. The Sclairtech process[®] uses 1-butene as a comonomer for density control, and is added directly and total solution flowrate containing the Ziegler-Natta catalytic complex [1, 2].

Due to the C_4H_8 purity needed in the reaction zone, an adsorption system removes impurities carried by de comonomer before it is blended with the solution to the polymer to be synthesized. The importance of having 1-butene with a purity as high as possible lies in the fact that the methyl ethyl ketone is a powerful poison agent for the catalytic complex for its Lewis base structures, that can cause active site reduction [3].

As it was mentioned in the upper paragraph, adsorption which is today the most widely used nonvapor-liquid technique for molecular separation in petroleum, natural gas and the petrochemical industry, can be used to selective concentration of one specific compound at the surface of a microporous solid (adsorbent) through attractive forces weaker than the chemical bonds. In this particular case, purify the comonomer flowrate of compounds like methyl ethyl ketone (C_4H_8O), produced elsewhere in the process [4].

To ensure the correct behavior of the purification system mentioned above, it is mandatory to know how the adsorption process works, and in this manner, keep the 1-butene flowrate as pure as possible. For this reason, an study of breakthrough will be performed in each of the two towers that conforms the purification system in order to find: how the kinetical parameter (K_t) and how adsorption capacity (Q_0) behaves as a function of time and initial methyl ethyl ketone concentration, a mathematical model that reproduces the breakthrough data (Thomas model) and finally the total adsorption capacity of each pack. The information founded will be applicable as a tool to predict the system behavior when basic variables are modified and have a better understanding of the comonomer purification process.

Experimental part

In order to quantify the concentration of C_4H_8O entering to the purification system, samples as a function of operational time (running hours), were taken upstream and downstream the two adsorption towers shown in the figure 1.

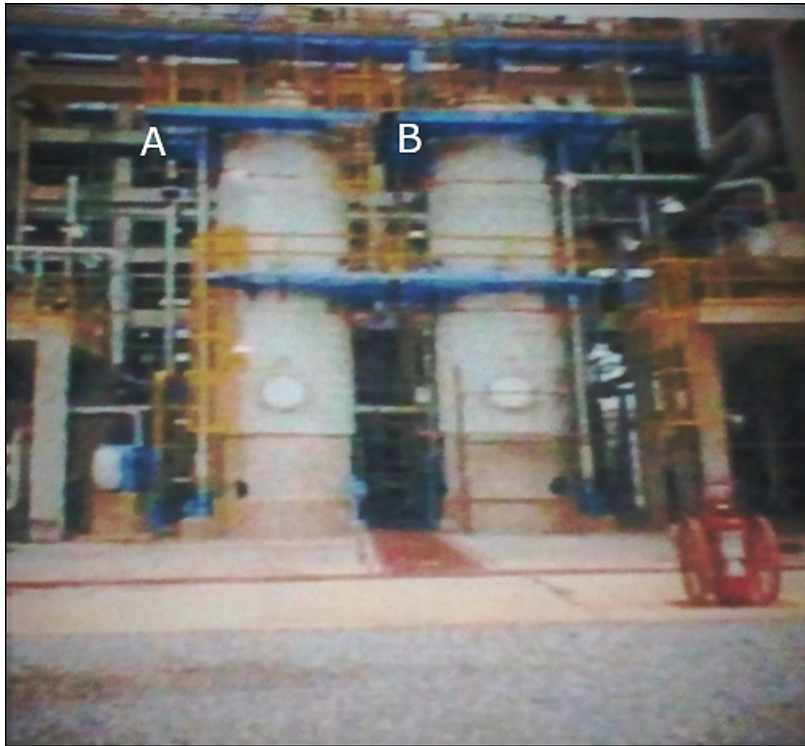


Figure 1. Adsorption towers chosen to build the breakthrough curves

The data collected in the towers was manipulated in order to present a graph of C_i/C_o against time of each purifier last in process (t_b), or the breakthrough curve for each purifier. In the same order of ideas, the Thomas model was chosen to fit the experimental outcomes and establish the kinetical parameter and the adsorption capacity for the towers. The equation (1), describes the model of Thomas:

$$\ln \ln \left(\frac{C_i}{C_o} - 1 \right) = \frac{K_L Q_o X}{Q} - \frac{K_L C_i V_{ef}}{Q} \tag{1}$$

Where: K_L is the rate constant for the process of adsorption, C_i the inlet C_4H_8O concentration, X the absorbent mass, Q_o the adsorption capacity, V_{ef} is the treated comonomer volume and Q is the volumetric flowrate.

In in a graph of the right part of equation (1) against the V_{ef} the slope of the curve could be used to establish the K_L and from the intercept of the same curve the adsorption capacity (Q_o). See the next two equations.

$$m = \frac{-K_L C_i V_{ef}}{Q} \tag{2}$$

$$AA = \frac{K_L Q_o X}{Q} \tag{3}$$

The total adsorbed mass of C_4H_8O can be calculated from equation (4)

$$QtQt = Q \int_{t=0}^{t=t_b} C_{ad} dt \tag{3}$$

And the total adsorption capacity of each pack can be obtained with equation (4)

$$Q_0 Q_0 = \frac{Q_t}{X} \quad (4)$$

Results

In the figure 2 the four breakthrough curves built with the data taken in the two towers can be observed.

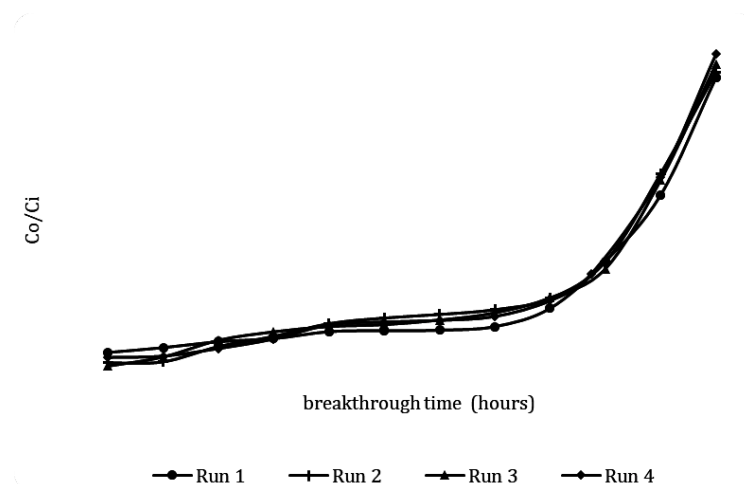


**Figure 2. Breakthrough runs for C₄H₈O adsorption over SiO₂.
Runs 1 and 2 purifier A Runs 3 and 4 purifier B.**

As can be seen, the four curves have a similar path, with an adsorption isotherm H1, corresponding to a mesoporous material. It is important to note that the four curves do not begin at the point of Co/Ci equal to zero, probably for the bad distribution of the comonomer flow [6, 7].

As the time passes, and as can be seen in the figure 2, the saturation of the mass transfer zones, happens in a very uniform way with weak tendency to increase the outlet concentration. When the operation times reach the 65 hours, the outlet concentration increase tendency become significant, this could be a signal that the mass transfer zone is approaching to the pack bottom or the adsorbent is depleted. Around 70 hours of run, the Co/Ci is equal to 0,5 and the pack is considered saturated [8, 9, 10].

Figure 3 show the fitting process of the four breakthrough curves to the Thomas model. As is widely known, the slope of the lineal manner of equation (1), can be used to calculate the mass transfer coefficient; and the intercept, as the slope, can be used to obtain the adsorption capacity both for the process of adsorption of C₄H₈O over SiO₂ [10].

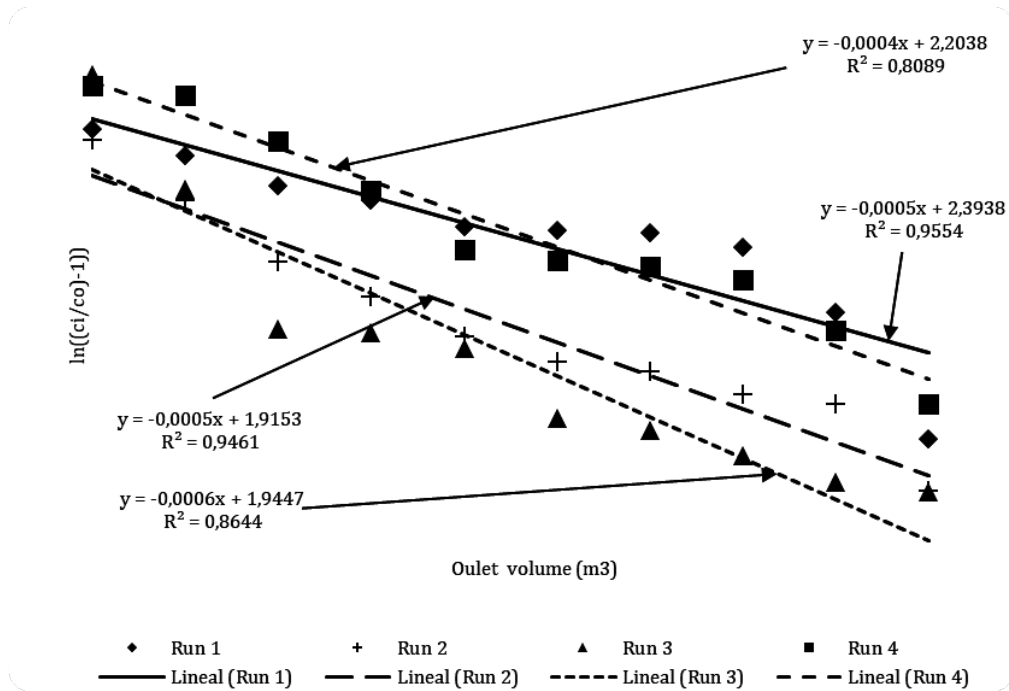


Figure 3. Fitting of breakthrough runs to Thomas model of C₄H₈O adsorption over SiO₂. Runs 1 and 2 purifier A Runs 3 and 4 purifier B.

In the next figure, can be observed the curve generated by the Thomas model joined with the experimental data taken the towers shown in the figure 1.

It can be seen clearly that Thomas model follows close the Ci/Co data from 0,1 to 0,25. For higher values of Ci/Co, the model does not follow the data tendency. Although, it is also reported that Thomas model is effective up to values of Ci/Co equals to 0,3 [5].

In the Thomas model it is assumed that the external and internal diffusion is not the limiting step, Langmuir kinetics of adsorption–desorption is valid and no axial dispersion is presented. However, adsorption is usually controlled by interphase mass transfer and the effect of axial dispersion could not be neglected, especially at a low flow rate. Such a discrepancy can result in errors when this model is used to predict column adsorption process, this could be the reason of the difference found between the data and the model when the values of Ci/Co are higher than 0,3 [5].

Another source of this discrepancy could be the existence of liquid maldistribution or Liquid channeling and wall flow for because the liquid takes the path of least resistance through the packing and forming flow channels for the individual phases, which are not necessarily in intimate contact with each surface allowing the methyl ethyl ketone pass through the bed without been taken by the actives sites of the adsorbent [11].

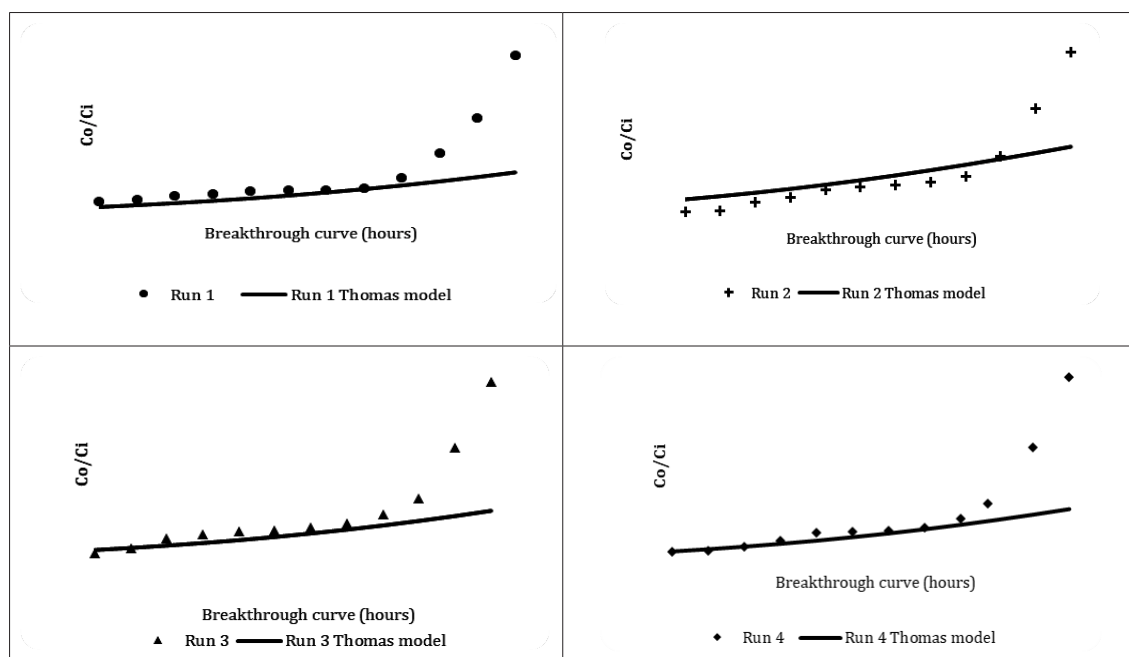


**Figure 4. Breakthrough curves fitted to Thomas model. Runs 1 and 2 purifier A
 Runs 3 and 4 purifier B.**

Using equations (2) and (3) in the figure 5 and 6 are presented the values of the mass transfer coefficient and the adsorption capacity both for the process of adsorption of C_4H_8O over SiO_2 .

In the first, place from figure 5 it could be observed the strong relationship between the mass transfer coefficient and the inlet methyl ethyl ketone concentration, for this reason when the concentration is low, the process has a big mass transfer, meaning a very low adsorption velocity. When the increase of the inlet concentration, the mass transfer coefficient reduces its value resulting in a rise of the adsorption process [5, 12].

It is important to highlight that when the inlet concentration is low the rate controlling process could be the migration of the methyl ethyl ketone from the bulk fluid to the surface particle, or external resistances to the mass transfer. When the concentration is high enough, in the case higher than 250 ppm a change in the mechanism is observed, and this could be attributed to an internal resistance to the mass transfer pore diffusion, inclusive, intraparticle diffusion [13-17].

It is normal to find more than one mass transfer rate in an adsorption process, and the domain one of them could be influenced by the concentration the adsorbing species. Deeper studies and comparative analysis will be necessary to determine mass transfer resistance for the adsorption [13-17].

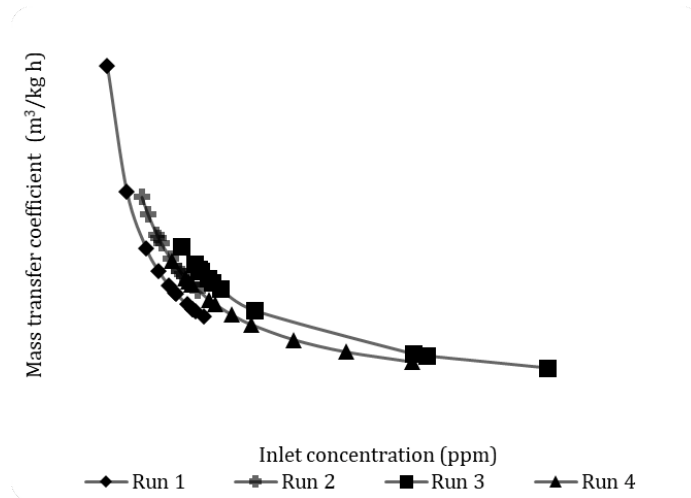


Figure 5. Global mass transfer coefficient as a function of the inlet concentration for the adsorption process of C_4H_8O over SiO_2 . Runs 1 and 2 purifier A Runs 3 and 4 purifier B.

The data shown in figure 6 reinforces what is already described and explained above, and it is: when the inlet concentration is low, the adsorption capacity is also low due to the high mass transfer coefficient, when the adsorption capacity rises, it is due to the diminution of the mass transfer coefficient for the increase in the inlet C_4H_8O concentration [12, 18, 19].

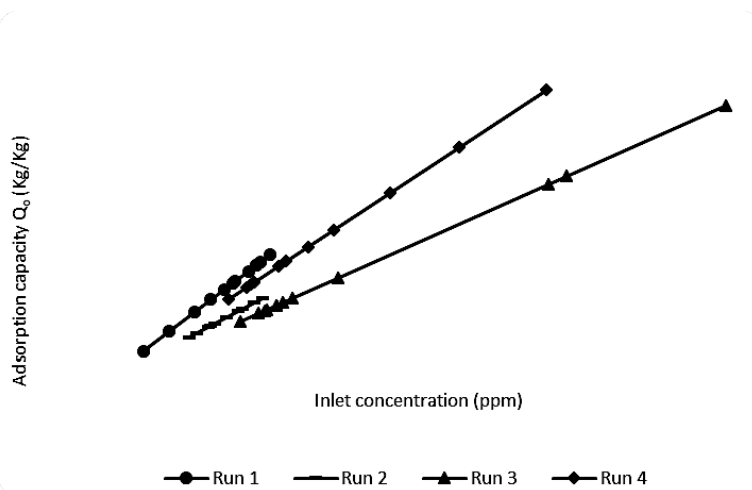


Figure 6. Adsorption capacity as a function of the inlet concentration, for the adsorption process of C_4H_8O over SiO_2 . Runs 1 and 2 purifier A Runs 3 and 4 purifier B.

Figure 7 shows the graph of ΔC as a function of time to in order to resolve numerically the equation (4), and with the use of equation (5), the adsorption capacity (C_o), can be obtained.

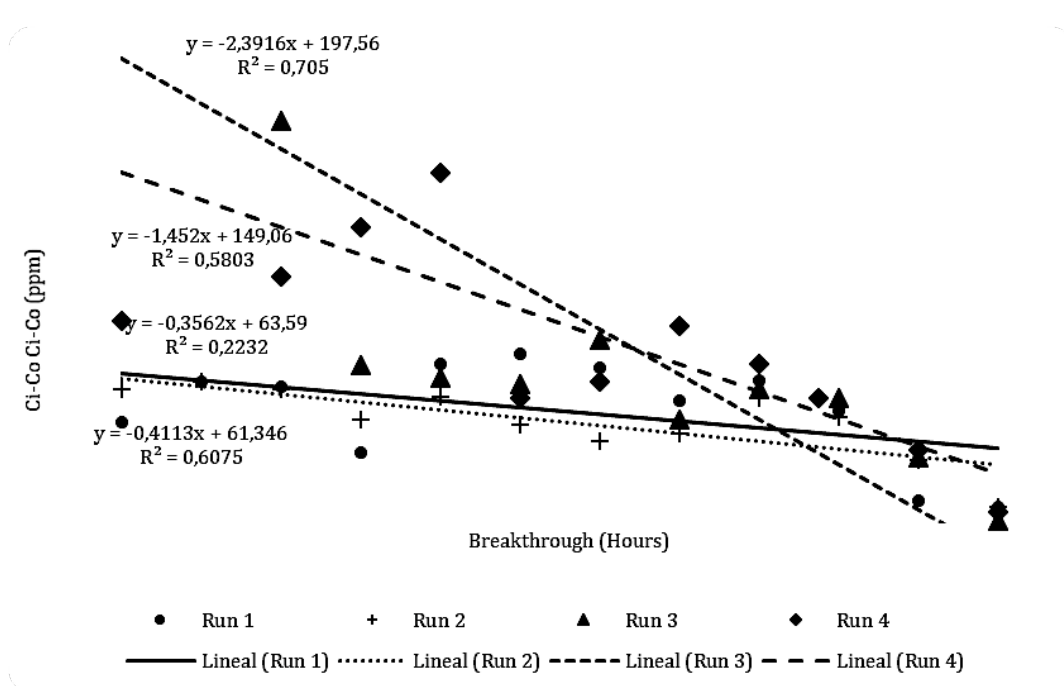


Figure 7. Fitting of ΔC as a function of time. Runs 1 and 2 purifier A Runs 3 and 4 purifier B.

In table 1 and using equation (3), (4) and (5), the pack adsorption capacity was established. It is important to highlight for the four runs, two for each tower, that they generated slightly different values of adsorption capacity, with tower A having the lowest values between the two packs. Although the uncertainty of the measurements leads us to assume the two packs have the same C_o .

Table 2. Adsorption capacities obtained by Thomas Model

Purifier	Run	Flowrate (m ³ /h)	Adsorbedmass (kg)	Adsorbent mass (Kg)	Adsorption capacity (Kg/Kg)
A	Run 1	42,8	252,1	9800	0,026
	Run 2	42,8	119,8	9800	0,019
B	Run 3	42,8	239,7	9800	0,025
	Run 4	42,8	248,5	9800	0,024

The manufacturer of the SiO₂ pack, provides the adsorption capacity for the solid, and its value can be between 0,01 and 0,05 kg/Kg [20, 21], and as can be seen, the values obtained in this study are between the given one, this leads us to assume that the Thomas method instead of the differences reported above, can be used to determinate the remaining adsorption capacity in adsorption packs with high use.

Conclusions

The Thomas model gave good agreement between experimental and calculated adsorption capacity and the Q_o given by the SiO₂ manufacturer, and can also be used to determinate the mass transfer coefficient and the adsorption capacity both, for the process of adsorption of C₄H₈O over SiO₂.

Attention must be paid in the differences obtained for higher values of Ci/Co, The Thomas model does not follow the data tendency, and that could be the cause of the low correlation coefficients in the fitting process shown in figure 7.

The migration of the methyl ethyl ketone from the bulk fluid to the surface particle, or external resistances to the mass transfer, can be the controlling stage in the adsorption process of C_4H_8O over SiO_2 .

Acknowledgments

The authors want to thank to Rafael Urdaneta University and Polinter, C.A, for their support during the execution of this work.

References

- [1] Malpass D., "Introduction to Industrial Polyethylene: Properties, Catalysts, Processes", John Wiley & Sons, New Jersey, 2010.
- [2] Hsieh E., Randall J. Ethylene-1-Butene copolymers. 1. Comonomer sequence distribution, *Macromolecules* vol (15), (1982) 353-360.
- [3] Tangjituabun K., Kim S., Hiraoka Y., Taniike T., Terano M. Poisoning of active sites on ziegler-natta catalyst for Propylene polymerization, *Chinese Journal of Polymer Science* vol 26 (5), (2008) 547-552.
- [4] Rousseau R. Handbook of separation process technology, John Wiley & Sons, New Jersey, 1987.
- [5] Wu J., Qing Yu H., Biosorption of 2,4-dichlorophenol from aqueous solutions by immobilized *Phanerochaete chrysosporium* biomass in a fixed-bed column, *Chemical Engineering Journal* vol 138, (2008) 128–135.
- [6] Sing K., Williams R. Physisorption hysteresis loops and the characterization of nanoporous materials, *Adsorption Science & Technology* vol 22 (4), (2004) 773-782.
- [7] Hanusch F., Rehfeldt S., Klein H. Liquid maldistribution in random packed columns: experimental investigation of influencing factors, *Chemical Engineering Technology* vol 89 (11), (2017) 1550–1560.
- [8] Miura A. Determination of cesium adsorption breakthrough curves using carbonized rice hull and beech sawdust as adsorbents, *Environment and Ecology Research* 5(6), (2017) 461-466.
- [9] Contreras J., Colina G., López D., Campos W., Rincón N. Adsorptive capacity of activated carbon from algarrobo as fixed bed for nickel adsorption, *Revista Técnica de la Facultad de Ingeniería Universidad del Zulia* vol 39 (1), 2016 24-30.
- [10] Patel H. Fixed-bed column adsorption study: a comprehensive review, *Applied Water Science* vol 9(45), (2019) 44-61.
- [11] Hanusch F., Rehfeldt S., Klein H. Liquid maldistribution in random packed columns: experimental investigation of influencing factors, *Chemical Engineering & Technology* vol 89 (11) (2017) 1550–1560.
- [12] Garcia C., Chavez G. Sistema $Cu^{++}Na^{+}$ dowex 50W-X8 en lecho fluidizado, vol 7 (1), (1984) 29-37.
- [13] McKay G., Blair H., Garner J. The adsorption of dyes in chitin. III. Intraparticle diffusion processes, *Journal of Applied Polymer Science* vol 28 (1983) 767-1778.

[14] Avramidis S. An investigation of the external and internal resistance to moisture diffusion in wood, *Wood Science and Technology* vol 28, (1987) 249-256.

[15] Fulazzaky A., Khamidun M., Omar R. Understanding of mass transfer resistance for the adsorption of solute onto porous material from the modified mass transfer factor models, *Chemical Engineering Journal* vol 228, (2013) 1023–1029.

[16] Chauveau R., Grévillet G., Marsteau S., Vallières C. Values of the mass transfer coefficient of the linear driving force model for VOC adsorption on activated carbons, *chemical engineering research and design* vol 91, (2013) 955–962.

[17] Koumanova B., Peeva P., Allen S. Variation of intraparticle diffusion parameter during adsorption of p-chlorophenol onto activated carbon made from apricot, of *Chemical Technology and Biotechnology* vol 78, (2003) 82–587.

[18] Rios J., Castellar G. Predicción de las curvas de ruptura para la remoción de plomo (II) en disolución acuosa sobre carbón activado en una columna empacada, *Revista Facultad de Ingeniería Universidad de Antioquia* vol 66, (2013) 141-158.

[19] Chowdhury Z., Zain S., Rashid A., Rafque R., Khalid K. Breakthrough curve analysis for column dynamics sorption of Mn(II) ions from wastewater by using Mangostana garcinia peel-based granular-activated carbon, *Journal of Chemistry* vol 2013, (2012) 1-8.

[20] Julio Moreno. Propuesta de mejoras al sistema de purificación de solvente/comonomero en una planta de polietileno lineal. Trabajo especial de grado. Facultad de ingeniería, Universidad Rafael Urdaneta, 2006.

[21] Zaida Borjas, Eulises Vargas. Optimización de los lechos secadores de etileno FF2002 A y B de la planta de polietileno lineal. Trabajo especial de grado. Facultad de ingeniería, Universidad Rafael Urdaneta, 2006.